*Desalination and Water Treatment*
www.deswater.com
4 (2009) 294–305
1944-3994/1944-3986 © 2009 Desalination Publications. All rights reserved

# Effect of various inorganic anions on the degradation of Congo Red, a di azo dye, by the photo-assisted Fenton process using zero-valent metallic iron as a catalyst

L. Gomathi Devi*, S. Girish Kumar, K. Mohan Reddy, C. Munikrishnappa

*Department of Post Graduate Studies in Chemistry, Central College City Campus, Dr. B.R. Ambedkar Veedi, Bangalore University, Bangalore 560 001, India*
*Tel. +91 80 2296 1336; email: gomatidevi_naik@yahoo.co.in*

Received 14 June 2008; Accepted 9 March 2009

**ABSTRACT**

The present research focuses on the heterogeneous advanced photo-Fenton processes of the type $Fe^0/H_2O_2/UV$ and $Fe^0$/ammonium persulfate (APS)/UV as a potential technique to degrade Congo Red (di azo dye). Both the oxidants $H_2O_2$ and APS showed comparable efficiencies on the iron surface for the mineralization of Congo Red (CR) under UV light. The influence of various reaction parameters like pH of the solution, catalyst loading, concentration of the oxidants ($H_2O_2$/APS), influence of hydroxyl radical scavenger and the concentration of the substrate dye molecules are investigated and the optimum conditions are reported. The influences of various inorganic anions that are commonly present in the industrial effluents are studied using the above processes. All the inorganic anions used shows inhibitive effect on the degradation rate. Inorganic anions like chloride ($Cl^-$) and sulfate ($SO_4^{2-}$) inhibit the degradation rate by forming complexes with $Fe^{2+}/Fe^{3+}$ ions in the solution and they also quench the generated hydroxyl radicals. Anions like nitrate ($NO_3^-$), carbonate ($CO_3^{2-}$) and bicarbonate ($HCO_3^-$) suppress the degradation rate mainly by scavenging the generated hydroxyl radicals. Quinol, hydroquinone and naphthalene derivative were the major intermediates obtained during the mineralization process. The experiments were extended successfully to treat the industrial effluent containing CR dye. APS proved to be a better oxidant than $H_2O_2$ for treating the effluent. The present method is advantageous as it is a simple and cost-effective technique for the mineralization of non-biodegradable di azo dye.

***Keywords***: Advanced oxidation process (AOP); Photo-Fenton type reaction; Zero-valent metallic iron surface; Inorganic anions; Congo Red

## 1. Introduction

Dye pollutants from textile industries are a major source of environmental pollution. The removal of these dyes from the wastewater is a challenging problem to the related industries, as these dyes are stable and difficult to destroy by conventional techniques. Traditional methods like flocculation, adsorption on activated carbon, reverse osmosis and activated sludge process have limitations and have further disadvantages as they transfer the pollutants from one phase to another phase rather than destroying them [1]. While ozone and hypochlorite oxidation process are efficient in the decolorization of the dyes, where decolorization refers to the destruction of the chromophore in the dye molecule which is responsible for its color and characteristic bands in the visible region of the spectrum, in the present case it refers to the destruction of two azo (-N=N-) bonds in the Congo Red (CR) molecule. It is measured by the extent of decrease in the peak intensity of $\lambda_{max}$ (577 nm). Complete destruction of these

*Corresponding author.

groups, leading to the formation of $CO_2$ and $H_2O$, is referred to as mineralization. Therefore, the above-mentioned techniques cannot be implemented due to the high cost of the equipment, and the secondary pollution, arising from the residual chlorine, limits their application. In the proposed advanced oxidation processes (AOPs), organic molecules are completely mineralized with the reactions involving hydroxyl radicals. Fenton's oxidation generates hydroxyl radicals from Fenton's reagent ($Fe^{2+}$/$H_2O_2$). Although these reactions have been known for more than a century [2], it was been reported as a method for wastewater treatment since the 1990s [3–10].

Hydroxyl radicals have one unpaired electron and are a strong, non-selective, highly reactive oxidant second only to elemental fluorine in the reactivity. The reactants, oxidizing agent and the catalyst are in the same liquid phase in the homogeneous photo-Fenton process. However, the use of $Fe^{2+}$ ions as a homogeneous catalyst has a significant disadvantage since it results in sludge formation (iron complexes). The method of removal of $Fe^{2+}$/$Fe^{3+}$ ions at the end of wastewater treatment is complicated, costly and requires a large amount of chemicals and man power [11]. In order to minimize the production of iron sludge in the homogeneous reaction, iron oxides such as magnetite($Fe_3O_4$), hematite ($Fe_2O_3$), goethite (FeOOH) or ferrihydrite ($Fe_5HO_8.4H_2O$) have been utilized instead of $Fe^{2+}$ ions [12].

Lucking et al. [13] emphasized the use of iron powder to replace iron ions as the catalyst in the Fenton/photo-Fenton reactions for the oxidation of 4-chlorophenol in aqueous solution with hydrogen peroxide. In the homogeneous photo-Fenton process, $Fe^{2+}$ ions are oxidized to $Fe^{3+}$ ions at a faster rate ($76\ M^{-1}s^{-1}$). But the back reduction of $Fe^{3+}$ ions is the rate-determining step that reduces the efficiency of the process ($3.33\times10^{-6}\ M^{-1}s^{-1}$) [14]. The limitation of the process is the non-reusability of the catalyst since separation of $Fe^{2+}$ ions is difficult. In the heterogeneous process the solid iron particles are more easily to be removed and recycled.

Zero-valent metallic iron (ZVMI) has been used as a potential catalyst for the efficient production of hydroxyl radicals in Fenton/photo-Fenton process to degrade many pollutants [15–22]. The use of metallic iron powder in the advanced Fenton process (AFP) initially generates $Fe^{2+}$ ions. These ions are further oxidized in the presence of oxidizing agents. The back-photo reduction reaction of $Fe^{3+}$ ions to $Fe^{2+}$ ions is much faster on the iron surface [Eq. (1)] compared to the homogeneous Fenton process [23].

$$2Fe^{3+} + Fe^0 \rightarrow 3Fe^{2+} \quad (1)$$

Iron powder under dissolution in acidic condition gives $Fe^{2+}$ ions by losing two electrons.

$$Fe^0 \rightarrow Fe^{2+} + 2e^- \quad (a)$$

In accordance with the classical Fenton reaction, $Fe^{2+}$ ions react with the electron acceptors ($H_2O_2$/APS) and are oxidized to $Fe^{3+}$ ions. The back reduction of $Fe^{3+}$ on the iron surface takes place according to the equation

$$Fe^{3+} + e^- \rightarrow Fe^{2+} \quad (b)$$

Since two electrons are available when iron powder undergoes dissolution as shown in Eq. (a), two $Fe^{3+}$ ions accept two electrons forming two $Fe^{2+}$ ions.

$$2Fe^{3+} + 2e^- \rightarrow 2Fe^{2+} \quad (c)$$

Summing up Eqs. (a) and (c), we get Eq. (1).

CR is a di azo dye. It is well known that di azo dyes are more difficult to degrade than mono azo dyes. Azo dyes are resistant to degradation under aerobic conditions [24]. Under anaerobic conditions they are reduced to potentially carcinogenic aromatic amines [25,26]. Accordingly, the present research work focuses on the process of degradation of synthetic dye CR using ZVMI of 300 mesh size as a source to generate $Fe^{2+}$ ions. Various inorganic salts (electrolytes) are used as additives in textile industries in order to improve color fastness on the fabric. A study involving the effects of inorganic anions on the photo-Fenton degradation will therefore be very useful for understanding the mechanism of the reaction. Therefore, the influence of $Cl^-$ (chloride), $CO_3^{2-}$ (carbonate), $HCO_3^-$ (bicarbonate), $SO_4^{2-}$ (sulfate) and $NO_3^-$ (nitrate) ions on the decolorization rates were studied. In addition, the methodology is extended to the textile effluent containing CR dye.

The effluents containing dyes are very difficult to treat since they contain many ingredients like detergents, oils, inorganic salts, heavy metals etc.; for such effluents the BOD/COD ratio will be high, implying non-biodegradability of the dye. The dyes found in the effluents come from different production lines like dying, washing, etc. Accordingly, the configuration of the dyes can vary significantly in the effluents based on the pH. The nature and the concentration of the effluents not only vary from industry to industry but also within a given processing plant. Therefore optimization conditions can vary. It was found that the industrial effluents needed high iron dosage for efficient mineralization. This research work proposes a new potential catalyst ZVMI for an efficient process of catalysis in the mineralization of azo dyes and also for the treatment of effluents containing these dyes.

## 2. Materials and methods

CR was supplied from Aldrich. It is commonly known as cotton red or direct red. The molecular formula of the

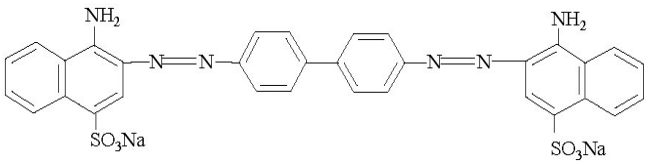


Fig. 1. Structure of Congo Red dye molecule.

dye is $C_{32}H_{22}N_6Na_2O_6S_2$ and molecular weight is 696.6. The molar extinction coefficient ($\varepsilon_{max}$) of CR is about 45,000 L $mol^{-1}cm^{-1}$. Hydrogen peroxide (50%) and ZVMI (300 mesh, electrolytic and 95% nominal purity) were supplied from S D Fine Chemicals, Bombay, and used without any pretreatment to iron. Sodium hydroxide, sulfuric acid and APS were of analytical grade chemicals. The structure of the dye is shown in Fig. 1.

### 2.1. Experimental set-up

Advanced photo-Fenton experiments were conducted using different reaction conditions: (1) variation in the pH of the solution, (2) variation in the concentration of the oxidants ($H_2O_2$ from 10 to 100 mg/L and APS from 50 to 250 mg/L); and (3) variation of iron dosage from 50 mg to 1000 mg/L. These experiments were planned in order to standardize and determine the optimum conditions required for dye degradation. An artificial light source of 125 W medium pressure mercury vapor lamp with a photon flux of 7.75 mW/$cm^2$ (as determined by ferri-oxalate actinometry) whose wavelength of emission is around 350–400 nm, was used [27,28]**.** The Pyrex glass reactor of size 150 × 75 mm with 1 L capacity whose surface area is 176 $cm^2$ was directly exposed to the light source in the presence of atmospheric oxygen. The entire photo reactor system was maintained at 25°C using a thermostat. The pH variation of the solution was adjusted either by adding dilute NaOH or $H_2SO_4$. In a typical experiment 25 mg/L of dye solution was used along with the desired amount of iron powder. The reaction mixture was stirred in the dark for 5 min. The light was focused on the solution at a distance of 29 cm and the oxidant $H_2O_2$/APS was added at the beginning of the experiment. The experimental set-up is shown in Fig. 2.

### 2.2. Analytical methods

The reaction solution (5 ml) was taken out from the reactor at definite time intervals and centrifuged. The centrifugate were analyzed by UV-visible spectroscopic technique using a Shimadzu UV-1700 Pharmaspec UV-visible spectrophotometer. The sample solution was extracted into non-aqueous medium and 1 $\mu$L was subjected to GC-MS analysis (using model GC-MS-QP-5000, Shimadzu) and a Thermo Electron Trace GC ultra coupled

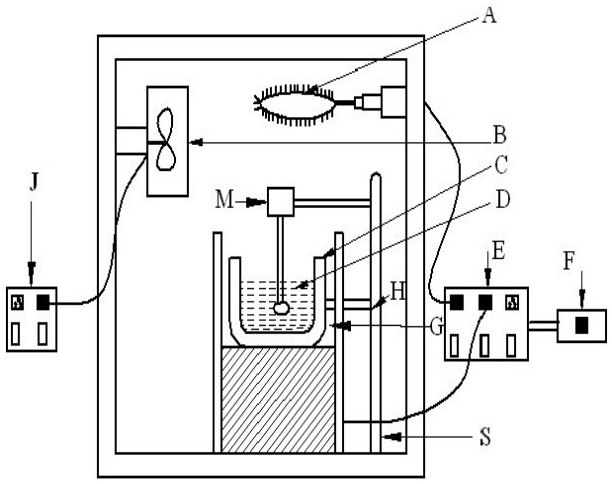


Fig. 2. Schematic diagram of the experimental set-up: (A) mercury vapor lamp; (B) fan; (C) Pyrex glass reactor; (D) experimental solution; (E) stabilizer; (F and J) switch box; (G) thermostat; (H) clamp; (M) motor; (S) stand.

to a DSQ mass spectrometer equipped with an Alltech Econo-Cap-EC-5 capillary column (30 m × 0.25 mm i.d × 0.25 mm film thickness) was used. Pure helium was used as the carrier gas at a flow rate of 1.2 ml/min. The injector/transfer line/trap temperature was 220/250/200°C respectively. Electron impact ionization was carried out at 70 eV.

## 3. Results and discussion

### 3.1. Comparison between Fenton and advanced photo- Fenton process

The various possible reactions taking place between the iron surface and the oxidants can be illustrated as follows:

Iron surface gets oxidized in acidic medium to form ferrous ions ($Fe^{2+}$).

$$Fe^0 \xrightarrow{H^+} Fe^{2+} + 2e^- \quad (2)$$

Alternatively $Fe^{2+}$ ions can also be generated by the reaction of iron surface with $H_2O_2$ that are partially adsorbed. Further, these adsorbed $Fe^{2+}$ ions can react with $H_2O_2$ leading to the generation of hydroxyl radicals.

$$Fe^0 + H_2O_2 \rightarrow Fe^{2+}\text{--surface} \quad (3)$$

$$Fe^{2+}\text{--surface} + H_2O_2 \rightarrow Fe^{3+} + OH^{\bullet} + OH^- \quad (4)$$

If these $Fe^{2+}$ ions are not partially adsorbed, they can diffuse into the bulk of the solution generating hydroxyl

anions. $Fe^0$ initially oxidizes to $Fe^{2+}$ by losing two electrons as shown in Eq. (5). Two electrons are transferred to electron acceptors like $H_2O_2$ which can form two hydroxide ions as shown in Eq. (6). On adding Eqs. (5) and (6), we get Eq. (7).

$$Fe^0 \xrightarrow{H^+} Fe^{2+} + 2e^- \quad (5)$$

$$H_2O_2 + 2e^- \rightarrow 2OH^- \quad (6)$$

$$Fe^0 + H_2O_2 \rightarrow Fe^{2+} + 2OH^- \quad (7)$$

The oxidant APS reacts with iron surface leading to the formation of sulfate and ferrous ions.

$$Fe^0 + S_2O_8^{2-} \rightarrow 2SO_4^{2-} + Fe^{2+} \quad (8)$$

The $Fe^{2+}$ ions can further react with the oxidant molecules generating free radicals by getting itself oxidized to $Fe^{3+}$ ions.

$$Fe^{2+} + H_2O_2 \rightarrow Fe^{3+} + OH^{\bullet} + OH^- \quad (9)$$

$$Fe^{2+} + S_2O_8^{2-} \rightarrow Fe^{3+} + SO_4^{2-} + SO_4^{\bullet-} \quad (10)$$

In Eq. (4), $Fe^{2+}$ ions are formed on the solid iron surface, which reacts with the oxidizing agent (rate constant is $6\times10^{-2}\ M^{-1}s^{-1}$), while in Eq. (9) it is the free $Fe^{2+}$ ions in the solution that react with the oxidants (rate constant is $76\ M^{-1}s^{-1}$). Though the nature of the products remains the same in both cases, the rate constant for the formation of $Fe^{3+}$ ions is higher [Eq. (9)] in the homogeneous condition [14].

Ferric ions ($Fe^{3+}$) so formed can react with molecules of water or $H_2O_2$ as represented in the following way:

(1) Ferric ions ($Fe^{3+}$) react with water to form an aqua complex. This complex under UV-irradiation generates $Fe^{2+}$ ions and hydroxyl radicals.

$$Fe^{3+} + H_2O \Leftrightarrow \left[Fe(OH)^{2+}\right] + H^+ \quad (11)$$

$$\left[Fe(OH)^{2+}\right] + h\nu \rightarrow Fe^{2+} + {}^{\bullet}OH \quad (12)$$

(2) $Fe^{3+}$ ions can also react with $H_2O_2$ leading to the formation of $Fe^{2+}$ ions along with hydro peroxyl radicals. Further these hydro peroxyl radicals so formed have the ability to reduce $Fe^{3+}$ ions, simultaneously generating hydroxyl radicals. The $Fe^{2+}$ ions are thus formed in two stages that participate actively in the cyclic Fenton reactions.

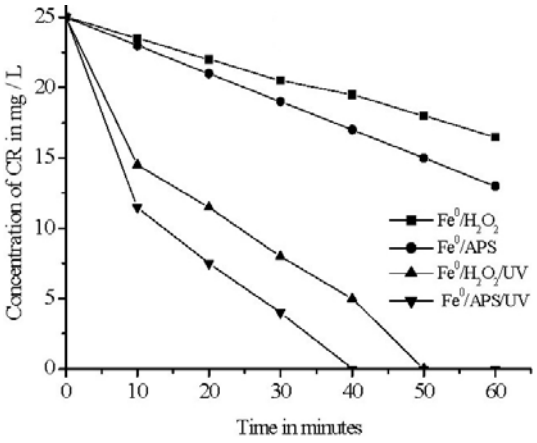


Fig. 3. Comparison of Fenton and photo-Fenton process for both oxidants. ($H_2O_2$ = 50 ppm, APS = 200 ppm, $Fe^0$ = 50 mg, dye = 25 mg/L and pH 3).

$$Fe^{3+} + H_2O_2 \rightarrow Fe^{2+} + {}^{\bullet}O_2H + H^+ \quad (13)$$

$$Fe^{3+} + {}^{\bullet}O_2H \rightarrow Fe^{2+} + {}^{\bullet}OH \quad (14)$$

Two molecules of sulfate radicals are produced when $Fe^{3+}$ ion reacts with persulfate anion, which can further react with water molecule generating hydroxyl radicals.

$$Fe^{3+} + S_2O_8^{2-} \rightarrow 2SO_4^{\bullet-} + Fe^{2+} \quad (15)$$

$$SO_4^{\bullet-} + H_2O \rightarrow SO_4^{2-} + {}^{\bullet}OH + H^+ \quad (16)$$

In order to determine the efficiency of the photo-Fenton process, the experiments were carried out in the dark. The plot of concentration vs. time shown in Fig. 3 implies the photo efficiency of the process. Only 50% and 44% of the dye was decolorized in the dark with $H_2O_2$ and APS as oxidants respectively in 1 h. The complete decolorization takes place in the presence of UV light more efficiently at a lesser duration. This is accounted for due to the back-reduction process of $Fe^{3+}$ to $Fe^{2+}$ (rate-determining step in the dark) taking place at a faster rate under UV illumination [29]. Photolysis of oxidants leading to the formation of various ions and radicals under UV light additionally contributes to the overall efficiency of the process.

### 3.2. *Effect of pH*

pH is an important parameter in the efficiency of the photo-Fenton process. It affects the formation and generation of hydroxyl radicals and pH also monitors the concentration of $Fe^{2+}$ ions in the solution. Kang et al. [30] reported that the pollutants can be decolorized efficiently

under acidic conditions rather than alkaline conditions. Many researchers have reported the optimum pH as 3 for the homogeneous photo-Fenton process. At this pH, the concentration of $Fe^{3+}$ ions and Fe $[OH]^{2+}$ complex ions is the dominating photo-active species in equal proportions. The change in this optimum pH leads to decrease in the concentration of Fe $[OH]^{2+}$ complex ions and it can also result in the precipitation of ferrous ion as oxy hydroxides. The various photo-active species of iron formed at different pH conditions can be summarized as: $Fe[H_2O]_6^{3+}$ (pH 1–2), Fe $[OH][H_2O]_5^{2+}$ (pH 2–3) and $Fe[OH]_2[H_2O]_4^{+}$ (pH 3–4) [31,32]. When the pH of the solution was increased from 2 to 3, the decolorization efficiency also increased from 44% to 100%. The decrease in the rate of decolorization of CR dye at low pH can be explained by the presence of excess $H^+$ ions in the solution which can act as a hydroxyl radical scavenger [Eq. (15)] [33].

$$H^+ + {}^{\bullet}OH + e^- \rightarrow H_2O \quad (17)$$

Beyond this optimum pH, decolorization efficiency is reduced. This is due to the aggregation or coagulation of $Fe^{3+}$ complex molecules formed in the reaction which inhibit the catalytic reaction of $Fe^{2+}$ ions with the oxidants. At high pH, precipitation of iron oxy hydroxides takes place that gets deposited on the iron powder, preventing the further process of generation of hydroxyl radicals [33]. Therefore, all the photo-Fenton experiments are most efficient at pH 3.

The two sites of protonation in the CR molecule are azo group (-N=N-) and the primary amine group ($-NH_2$). In the complete range of pH there exists an equilibrium between the azo form (-N=N-) and the azonium ion ($-NH^+$= N-). Since the efficient degradation of the dye takes place at pH 3, it is assumed that the concentration of azonium ions was appreciably higher than the azo species and it undergoes degradation in the photo-Fenton reaction. The protonation of amine gives rise to ammonium ion ($-NH_3^+$) which do not have any effect on the reactivity of azo group or on the degradation rate.

### 3.3. Effect of catalyst loading

The optimization of the catalyst is a necessary step in the photo-Fenton reaction mechanism**.** In the presence of oxidant alone, the decolorization efficiency was found to be 62 and 47% respectively with $H_2O_2$ and APS. This is due to the direct photolysis of oxidants in the presence of UV light. However, complete decolorization with higher efficiency was achieved by the use of iron surface in the presence of oxidants (Fig. 4). The iron surface catalytically decomposes the oxidants to respective free radicals/ions more efficiently under UV light. On the contrary, over-

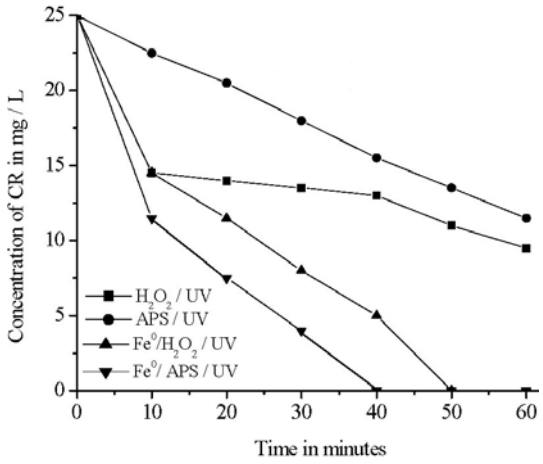


Fig. 4. Degradation of CR with and without catalyst in the presence of oxidants and UV light. ($H_2O_2$ = 50 ppm, APS = 200 ppm, $Fe^0$ = 50 mg, dye = 25 mg/L and pH 3).

loading of the catalyst hinders the decolorization efficiency. This may be due to: (1) higher concentration of the catalyst results in turbidity which hinders UV light penetration [34]; (2) with increase in the catalyst concentration, the final pH of the solution increases, which in turn adversely affects the decolorization rate. When the catalyst loading is 50 mg/L, the final pH of the reaction mixture is 3.5. With further increase in the catalyst concentration to 150 mg/L, pH of the solution changes to 4.4, leading to the yellow coloration. At this condition, turbidity in the reaction mixture is observed. On further increase in the catalyst loading (250–1000 mg/L), excess iron precipitates as iron oxy hydroxides and the precipitate separates from the true solution and the pH of the solution changes to 4.9. Moreover, high dosage of iron powder increases the concentration of $Fe^{2+}$ ions in the solution which can also act as hydroxyl radical scavenger [Eq. (16)] [33].

$$Fe^{2+} + {}^{\bullet}OH \rightarrow Fe^{3+} + OH^- \quad (18)$$

### 3.4. Effect of oxidants

The present study investigates the application of HOOH (hydrogen peroxide) and $S_2O_8^{2-}$ (peroxy disulfate) which are symmetrical peroxides and can be potential oxidants in the light induced reaction processes. Persulfate can also generate free radicals like sulfate and hydroxyl radicals which provide free radical mechanism similar to hydroxyl radical pathways generated in Fenton's chemistry. The sulfate radical is one of the strongest oxidizing species in aqueous media with a redox potential of 2.6 V. It is next only to the hydroxyl free radical whose redox potential is 2.8 V. In addition to its oxidizing strength, the persulfate and sulfate radicals have several advantages

over the other oxidant systems: (1) sulfate radicals are kinetically fast; (2) sulfate radicals are more stable and are able to transport efficiently on the solid surface compared to hydroxyl radicals; (3) persulfate provides better acidic pH, hence an efficient electron acceptor capable of accelerating the mineralization process. The sulfate radical anions produced in the case of APS show various possible reaction mechanisms in the process of mineralization: (1) abstraction of hydrogen atom from the saturated carbon; (2) ability to add to the unsaturated compounds; (3) removal of an electron from the anions and neutral molecules [35,36]. These attributes combine to make persulfate a viable option for the chemical oxidation of a broad range of contaminants.

The influence of oxidants on the degradation was investigated by maintaining the other reaction parameters constant: 0.5 ml of 50% $H_2O_2$ solution in 1 L, resulting in 50 ppm, was used as stock solution. It can be seen from Fig. 5a that with an increase in the concentration of $H_2O_2$ (from 10 mg to 50 mg/L), the decolorization efficiency increased from 46% to 100%. With a further increase in the concentration of oxidant, the efficiency of the process decreases. This can be due to the recombination of the excess hydroxyl radicals generated or it might get involved in the unwanted reaction pathways. Similar experiments were carried with APS (1 mg of APS in 1 L results in 1 ppm), and its optimum concentration was found to be 200 mg/L (Fig. 5b).

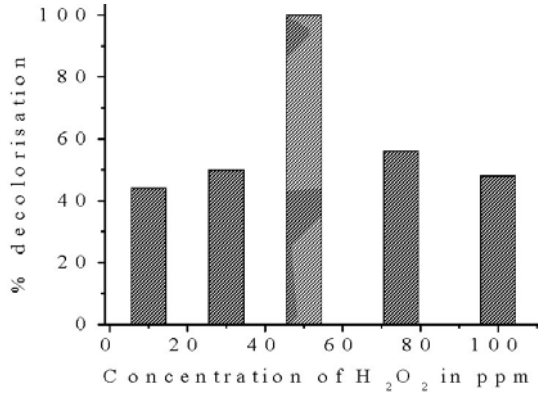


Fig. 5a. Plot of concentration of CR vs. time for different concentrations of $H_2O_2$ as oxidant. ($H_2O_2$ = 10–100 ppm, $Fe^0$ = 50 mg, dye = 25 mg/L and pH 3).

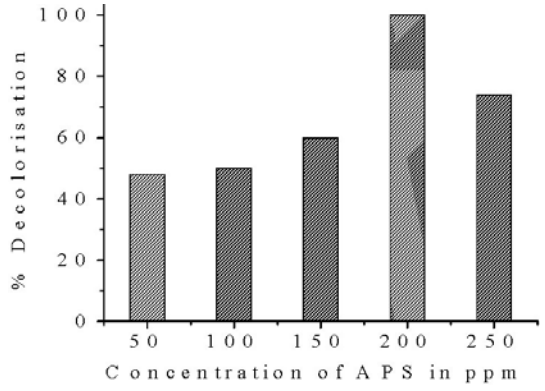


Fig. 5b. Plot of concentration of CR vs. time for different concentrations of APS as oxidant. (APS = 50–250 ppm, $Fe^0$ = 50 mg, dye = 25 mg/L and pH 3).

### 3.5. Effect of initial concentration of the dye

In the photo-Fenton process, change in the dye concentration affects the degradation process significantly. Therefore, experiments were performed at different initial dye concentrations by maintaining the other reaction parameters constant. The calculated values of % decolorization, rate ($d\alpha/dt$) and the process efficiency ($\Phi$) for different initial concentrations of the dye along with the oxidants are shown in the Table 1. The calculated values of process efficiency ($\Phi$) imply the effectiveness of the present method. The process efficiency can be defined as the residual concentration divided by the amount of energy in terms of intensity and exposure surface area per time.

$$\Phi = \frac{C_0 - C}{t.I.S} \tag{19}$$

where $C_0$ is the initial concentration of the dye substrate and $C$ is the concentration at time $t$ and ($C_0 - C$) denotes the residual pollutant concentration in mg/L or ppm; $I$ is the irradiation intensity, 125 W; $S$ denotes the solution irradiated plane surface area in $cm^2$; and $t$ represents the irradiation time (min).

The performance of catalysis is characterized by the process efficiency. The essential need of the catalyst and its active role is also depicted in the process efficiency; % decolorization and the rate show parallel variations with process efficiency. Beyond the optimum concentration (25 mg/L), the % decolorization decreases to 16% for higher initial dye concentration. This may be due to the fact that, as the dye concentration is increased, the number of hydroxyl radicals is not in-creased proportionally. High dye concentration prevents the UV light penetration into the depth of the solution, thereby decreasing the generation of hydroxyl radicals [37]. Moreover, at high concentrations, the active centers on the iron surface will be occupied by the dye molecules which are capable of reducing the catalyst surface itself by hindering the further process of generation of hydroxyl radicals. The calculated rates and the process efficiencies confirm the effectiveness of the advanced Fenton process at lower concentration of the dye.

Table 1
Percent decolorization, rate (dα/d*t*) and process efficiency (Φ) for different initial concentrations of dye

| Advanced Fenton process | [C] of the dye (mg/L) | % decolorisation | Rate (dα/dt) ($\times10^{-2}$ $min^{-1}$) | Process efficiency (Φ) ($\times10^{-9}$ ppm $min^{-1}$ $W^{-1}$ $cm^{-2}$) |
|---|---|---|---|---|
| $Fe^0$/UV/ APS | 25 | 100 | 1.4 | 2.11 |
| | 40 | 66 | 1.1 | 1.47 |
| | 50 | 69 | 0.6 | 1.56 |
| | 75 | 16 | 0.2 | 1.01 |
| $Fe^0$/UV/$H_2O_2$ | 25 | 100 | 1.2 | 1.69 |
| | 40 | 57 | 1.0 | 1.28 |
| | 50 | 67 | 0.9 | 1.21 |
| | 75 | 16 | 0.3 | 1.01 |

Table 2
Percent decolorization, rate (dα/d*t*) and process efficiency (Φ) in presence and absence of methyl alcohol for optimized experiments

| Advanced Fenton process | % decolorisation | | Rate dα/d*t* ($\times10^{-2}$ $min^{-1}$) | | Process efficiency (Φ) ($\times0^{-9}$ ppm $min^{-1}$ $W^{-1}$ $cm^{-2}$) | |
|---|---|---|---|---|---|---|
| | Without $CH_3OH$ | With $CH_3OH$ | Without $CH_3OH$ | With $CH_3OH$ | Without $CH_3OH$ | With $CH_3OH$ |
| $Fe^0$/UV/$H_2O_2$ | 100 | 64 | 1.2 | 0.4 | 1.69 | 1.01 |
| $Fe^0$/UV/APS | 100 | 76 | 1.4 | 0.4 | 2.11 | 1.35 |

### *3.6. Effect of hydroxyl radical scavenger*

The role of hydroxyl radicals in the oxidation of azo dye by photo Fenton process was confirmed by carrying the degradation process in the presence of hydroxyl radical scavenger like methyl alcohol. Methyl alcohol is known to deactivate hydroxyl radical and its derivatives [36]. Methanol reacts with hydroxyl radical and to a lesser extent with hydrogen radical whose second-order rate constants are $9.7\times10^8$ $mol^{-1}$ $s^{-1}$ and $2.6\times10^6$ $mol^{-1}$ $s^{-1}$ respectively [Eqs. (18) and (19)].

$$CH_3OH + {}^{\bullet}OH \rightarrow CH_3O^{\bullet} + H_2O \quad (20)$$

$$CH_3OH + {}^{\bullet}H \rightarrow CH_3O^{\bullet} + H_2 \quad (21)$$

The rate, process efficiency (Φ) and the % decolorization efficiency in the presence and absence of methyl alcohol are shown in Table 2. Color removal is 100% in the the absence of methyl alcohol. The efficiency decreased to 64% and 76% for 1 h of irradiation in the presence of methyl alcohol with $H_2O_2$ and APS as oxidants (Fig. 6). The decreasing effect is more for $H_2O_2$ compared to the APS. This is due to the inability of methyl alcohol to deactivate sulfate radicals, which mediates the degradation in the absence of hydroxyl radicals. Neta et al. [35] reported that sulfate radicals participate in the degradation either by electron abstraction or by adding to unsaturated atoms. These results provide evidence for the role of hydroxyl radicals in the degradation mechanism.

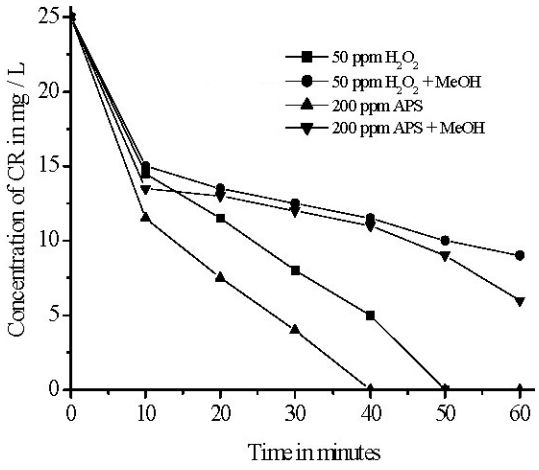


Fig. 6. Plot of concentration of CR vs. time for different oxidants in the presence of hydroxyl radical scavenger. ($H_2O_2$ = 50 ppm, APS = 200 ppm, $Fe^0$ = 50 mg, dye = 25 mg, $CH_3OH$= 5 ml/L and pH 3).

### *3.7. Effect of various inorganic anions on decolorization*

The effect of inorganic anions on the % decolorization is shown in Tables 3 and 4 for APS and $H_2O_2$. It can be

Table 3
Percent decolorization, linear regression factor ($R^2$), rate ($d\alpha/dt$) and process efficiency ($\Phi$) in the presence of various inorganic anions for the advanced Fenton process ($Fe^0/APS/UV$)

| Ions $Fe^0/APS/UV$ | $d\alpha/dt$ ($min^{-1}$) $\times10^{-2}$ (at 30 min) | $R^2$ linear (from concentration vs. time plot) | Percent degradation | Process efficiency ($\Phi$) ($\times10^{-9}$ ppm $min^{-1}$ $W^{-1}$ $cm^{-2}$) |
|---|---|---|---|---|
| No salt | 1.4 | 0.8854 | 100 | 2.11 |
| $Cl^-$ = 0.01 M | 0.4 | 0.7191 | 44 | 0.92 |
| $Cl^-$ = 0.1 M | 0.2 | 0.6844 | 48 | 1.05 |
| $NO_3^-$ = 0.01 M | 0.4 | 0.6237 | 48 | 1.05 |
| $NO_3^-$ = 0.1 M | 0.4 | 0.8506 | 50 | 0.80 |
| $SO_4^{2-}$ = 0.01 M | 0.6 | 0.6587 | 62 | 1.30 |
| $SO_4^{2-}$ = 0.1 M | 1.0 | 0.8570 | 66 | 1.39 |
| $CO_3^{2-}$ = 0.01 M | 0.2 | 0.6743 | 40 | 0.84 |
| $CO_3^{2-}$ = 0.1 M | 1.4 | 0.8279 | 100 | 2.11 |
| $HCO_3^-$ = 0.01 M | 0.2 | 0.7310 | 46 | 0.97 |
| $HCO_3^-$ = 0.1 M | 1.4 | 0.8570 | 100 | 2.11 |

Table 4
Percent decolorization, linear regression factor ($R^2$), rate ($d\alpha/dt$) and process efficiency ($\Phi$) in the presence of various inorganic anions for the advanced Fenton process ($Fe^0/H_2O_2/UV$)

| Ions $Fe^0/H_2O_2/UV$ | $d\alpha/dt$ ($min^{-1}$) $\times10^{-2}$ (at 40 min) | $R^2$ linear (from concentration vs. time plot) | Percent degradation | Process efficiency($\Phi$) ($\times10^{-9}$ ppm $min^{-1}$ $W^{-1}$ $cm^{-2}$) |
|---|---|---|---|---|
| No salt | 1.2 | 0.9419 | 100 | 1.69 |
| $Cl^-$ = 0.01 M | 0.2 | 0.6462 | 56 | 0.70 |
| $Cl^-$ = 0.1 M | 0.2 | 0.5576 | 36 | 0.54 |
| $NO_3^-$ - = 0.01 M | 1.0 | 0.7809 | 58 | 0.98 |
| $NO_3^-$ = 0.1 M | 0.8 | 0.8679 | 50 | 0.84 |
| $SO_4^{2-}$ = 0.01 M | 0.6 | 0.8283 | 42 | 0.77 |
| $SO_4^{2-}$ = 0.1 M | 0.2 | 0.5901 | 48 | 0.81 |
| $CO_3^{2-}$ = 0.01 M | 0.2 | 0.5666 | 48 | 0.81 |
| $CO_3^{2-}$ = 0.1 M | 1.2 | 0.8505 | 100 | 1.69 |
| $HCO3^{-}$ = 0.01 M | 0.6 | 0.7291 | 46 | 0.77 |
| $HCO_3^-$ = 0.1 M | 0.2 | 0.6500 | 54 | 0.91 |

seen that the presence of all these anions investigated affects the decolorization efficiency adversely but only differs in their magnitude. The trend in rate of decolorization of the dye is different for different oxidants, and it also varies with the concentration (0.05 M and 0.5 M) of anions. Specifically, at lower concentrations of anions, the decolorization rate is affected in the following increasing order: $CO_3^{2-} > Cl^- > HCO_3^- > NO_3^- > SO_4^{2-}$ for APS as oxidant. The decolorization rate is least affected by sulfate radicals at lower concentrations. But for higher concentrations of anions, the order is modified to $Cl^- > NO_3^- > SO_4^{2-} > CO_3^{2-} \approx HCO_3^-$. Similarly, for $H_2O_2$ as an oxidant, at lower concentrations of anions, the order is $SO_4^{2-} > HCO_3^- > CO_3^{2-} > Cl^- > NO_3^-$, while at higher concentrations of anions the order is changed to $Cl^- > SO_4^{2-} > NO_3^- > HCO_3^- > CO_3^{2-}$.

Higher concentrations of carbonate anions had no effect on the decolorization rate for either oxidant. The extent of quenching of hydroxyl radicals by the inorganic anions depends mainly on its concentration. There is an optimum concentration at which these anions quench the hydroxyl radicals to a maximum extent, beyond which it may not show any effect for the quenching of free radicals. The rate of the reaction ($d\alpha/dt$), linear regression factor ($R^2$) and the process efficiency ($\Phi$) calculated in the presence of various inorganic anions for both the oxidants are shown in Tables 3 and 4. The decrease in these parameters shows the extent of influence of anions on the decolorization rate. The $R^2$ value for the plot of concentration vs. time gives the extent of linearity. As the value of $R^2$ decreases, the plot deviates from the linearity, implying the deviation of the reaction from the first order. The observed deviation from the unity is more for the reactions in the presence of inorganic anions. From the results it can be concluded that, even in the presence of various inorganic anions, APS is found to be more efficient in the decolorization process than $H_2O_2$. This confirms the

fact that sulfate radicals can also mediate the degradation process along with the hydroxyl radicals. The effect of various inorganic anions on photo-Fenton degradation can be explained through the following proposed mechanisms.

*3.7.1. Effect of chloride*

Chlorides are known to form complexes with $Fe^{2+}$ and $Fe^{3+}$ ions in the solution which affect their equilibrium concentration [Eqs. (22)–(24)], thus reducing the generation of hydroxyl radicals in the cyclic Fenton reactions [38–40].

$$Fe^{3+} + Cl^- \rightarrow FeCl^{2+} \quad (22)$$

$$Fe^{2+} + Cl^- \rightarrow FeCl_2^+ \quad (23)$$

$$FeCl_2^+ + Cl^- \rightarrow FeCl_3 \quad (24)$$

In addition, the chloride anion can also scavenge the hydroxyl radicals [Eq. (25)}:

$$Cl^- + {}^{\bullet}OH + H^+ \rightarrow Cl^{\bullet} + H_2O \quad (25)$$

*3.7.2. Effect of nitrates, bicarbonates and carbonates*

Nitrates, bicarbonates and carbonates do not form complexes with either $Fe^{2+}$ or $Fe^{3+}$. Therefore, the reaction between iron ions and oxidants is not suppressed. The main mechanism for their inhibitive effect on dye decolorization can be due to scavenging effect of hydroxyl radicals generated from photolysis of oxidants [40,41]. In the presence of $H_2O_2$, nitrate acts as an "inner filter" and reduces the UV light intensity in the photo reactor. Nitrate can also absorb UV light at shorter wavelengths, thereby reducing the number of photons reaching the solution [42]. The possible reactions of nitrate, carbonate and bicarbonate ions with hydroxyl radicals can be proposed as shown in Eqs. (26)–(28):

$$NO_3^- + {}^{\bullet}OH \rightarrow NO_3^{\bullet} + OH^- \quad (26)$$

$$CO_3^{2-} + {}^{\bullet}OH \rightarrow CO_3^{-\bullet} + OH^- \quad (27)$$

$$HCO_3^- + {}^{\bullet}OH \rightarrow CO_3^{-\bullet} + H_2O \quad (28)$$

*3.7.3 Effect of sulfate*

Sulfate can form a complex with both $Fe^{2+}$ and $Fe^{3+}$ ions and it can also act as an hydroxyl radical scavenger [40] [Eqs. (29)–(32)]:

$$Fe^{2+} + SO_4^{2-} \rightarrow FeSO_4 \quad (29)$$

$$Fe^{3+} + SO_4^{2-} \rightarrow FeSO_4^+ \quad (30)$$

$$Fe^{3+} + 2SO_4^{2-} \rightarrow Fe(SO_4)_2^- \quad (31)$$

$$SO_4^{2-} + {}^{\bullet}OH \rightarrow SO_4^{-\bullet} + OH^- \quad (32)$$

*3.8. UV-visible spectroscopy*

The color of CR dye is sensitive to the changes in the pH of the medium. The dye molecule is characterized by the peak at 497 nm in the visible region due to the azo form. The second peak at 340 nm in the UV region is attributed to the naphthalene rings in the dye structure. The third and fourth peaks at 268 and 246 nm are due to the benzene rings in the molecule. On protonation, especially at pH 3, the intense band (497 nm) shows a red shift to 577 nm due to the formation of azonium ion. The peak at 268 nm shows a slight red shift to 284 nm due to the resonance modification of the π system in the structure, while the peak at 340 nm and 246 nm shows a blue shift. On irradiation along with iron powder and $H_2O_2$, the band at 577 nm reduces its intensity and completely diminishes at 50 min, confirming the decolorization of the dye. This suggests that degradation proceeds through the cleavage of the azo chromophore (which is also identified in the GC-MS technique). The intensity of the bands 220 and 340 nm increases due to the formation of stable intermediate products corresponding to aromatic and naphthalene derivatives. All the peaks completely disappear by 2 h of irradiation (Fig. 7). However, complete mineralization of the dye takes 2.5 h. From spectroscopic analysis it can be concluded that both oxidants show a comparable oxidizing capacity.

*3.9. GC-MS analysis*

The intermediates formed during the process of degradation are confirmed by GC-MS analysis. The GC-

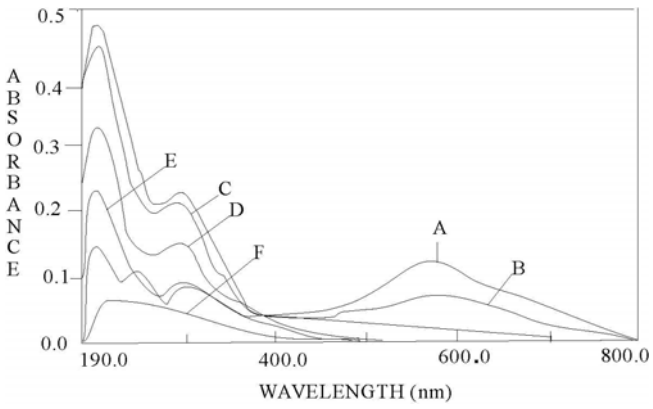


Fig. 7. UV-visible spectra for the degradation of CR by the advanced Fenton process. (Iron powder = 50 mg, APS = 200 ppm, pH = 3, dye = 25 mg/L). A, before irradiation. B, at 20 min. C, at 40 min. D, at 90 min. E, at 120 min. F, at 150 min.

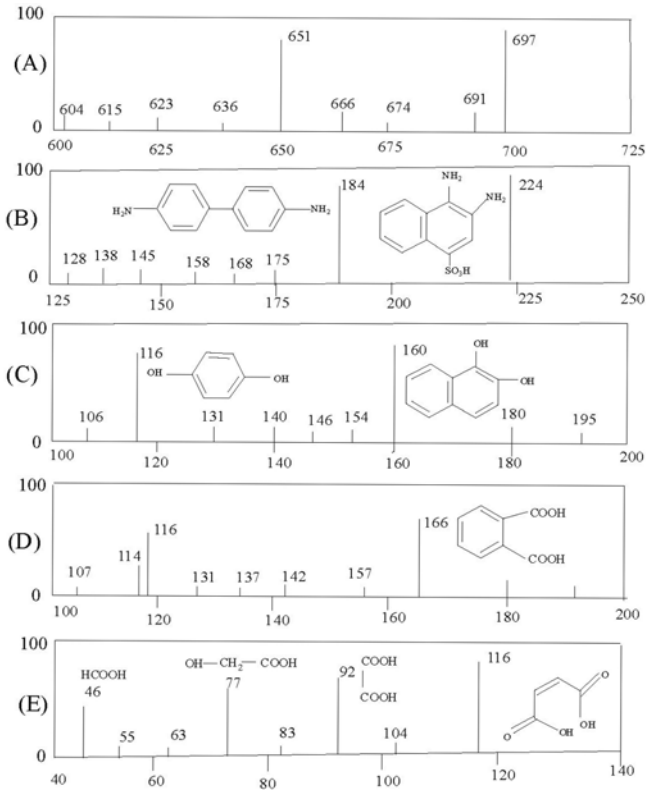


Fig. 8. The m/z spectra for the degradation of CR by the advanced Fenton process. (Iron powder = 50 mg, APS = 200 ppm, pH = 3, dye = 25 mg/L). A, initial dye spectrum. B, at 50 min. C, at 75 min. D, at 90 min. E, at 150 min.

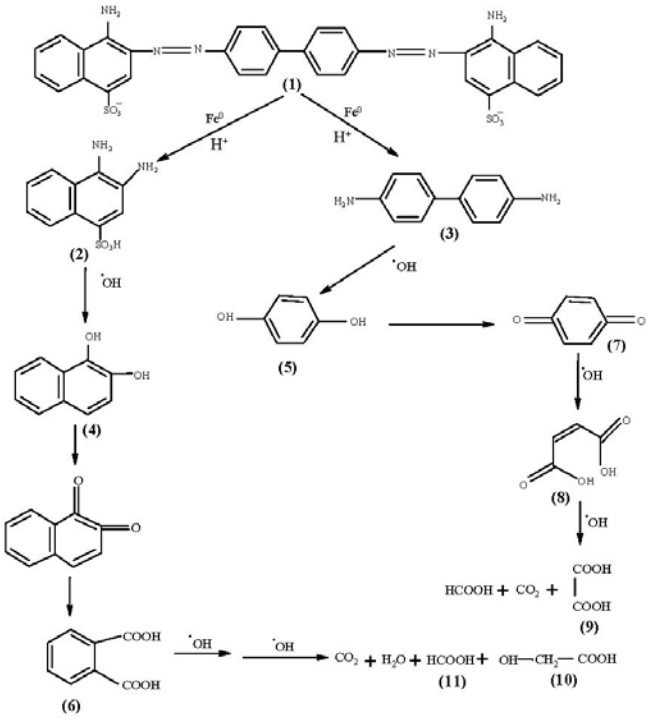

Fig. 9. Probable degradation mechanism of CR.

MS spectra recorded for the CR solution show m/z peaks at 651 of medium intensity corresponding to the ionized dye molecule (1) (Fig. 8). The m/z peaks at 224 and 184 of high intensity appears due to the reduction of two azo bonds by the ZVMI corresponding to the 1, 2 di amino naphthalene sulphonic acid (2) and amine substituted bi phenyl compound (3) at 50 min of irradiation. The other lower intensity peaks at 154, 103 and 157 were not considered. At 75 min the major intermediates are m/z peak at 160 corresponding to di hydroxy substituted naphthalene (4) and m/z peak at 116 corresponding to quinol (5). At 90 min of irradiation m/z peaks of medium intensity at 166, 116 and 114 were found. The m/z peak at 166 can be assigned to pthalic acid (6) which is formed from the oxidation of di hydroxy substituted naphthalene to naptha quinone which further cleaves to form pthalic acid [43,44]. The m/z peak at 116 of low intensity corresponds to quinol and 114 to hydroquinone (7), resulting from the oxidation of quinol. At 2 h of irradiation the m/z peak at 116 of hydroquinone still persisted. At 2.5 h of irradiation m/z peaks at 116, 92, 77 and 46 of medium intensity, corresponding to maleic acid (8), oxalic acid (9), glyoxalic acid (10) and formic acid (11), were found as intermediates resulting from the cleavage of hydroquinone. Based on the above intermediates, a probable degradation mechanism is proposed in Fig. 9.

### *3.10. Treatment to effluent containing CR dye*

The optimized process was extended to industrial effluent containing CR dye. Effluent so obtained was filtered using Whatman filter paper to separate solid particles and was diluted appropriately. As discussed earlier, the inorganic ion forms complexes with iron ions, thereby inhibiting the generation of hydroxyl radicals from Fenton's reaction. Therefore, the treatment of effluent containing CR dye (25 mg/L) required a higher dosage of iron for its degradation.

The standardized experimental conditions are found to be inefficient in the treatment of effluent. With an increase in the iron dosage to 100 mg/,L decolorization of the effluent containing CR dye was completed by 1–1.5 h for both oxidants. When the iron dosage was increased to 200 mg/L, the decolorization efficiency increased for both oxidants, but precipitation of the excess iron as iron oxy hydroxides resulted during the course of the reaction and the final pH of the solution reached 5.3. Therefore, iron dosage was optimized to 100 mg/L for treating the effluents.

APS proved to be a better oxidant than $H_2O_2$ for treating industrial effluent as the sulfate radicals produced mediate the degradation along with hydroxyl radicals. The degradation of effluent was followed by UV-visible spectroscopy.

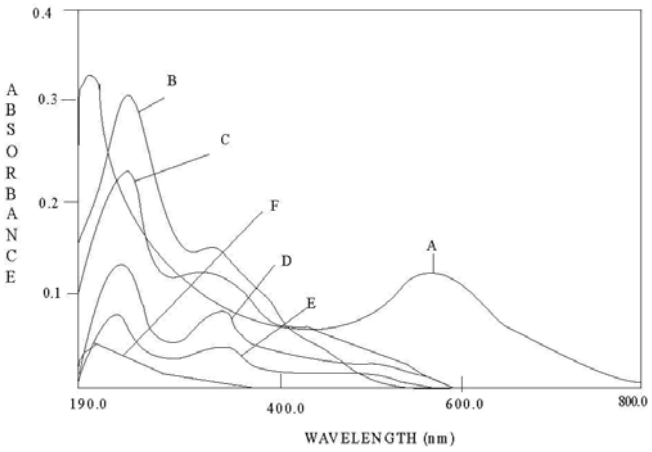


Fig. 10. UV-visible spectra for the degradation of effluent containing CR by the advanced Fenton process. (Iron powder = 100 mg, APS = 200 ppm, pH = 3, dye = 25 mg/L). A, before irradiation. B, at 90 min. C, at 120 min. D, at 180 min. E, at 240 min. F, at 300 min.

### *3.11. UV-visible spectral analysis of the effluent*

Fig. 10 shows the UV-visible spectra of the effluent containing CR dye. In the case of effluent, CR dye was characterized by a strong intense band at 562 nm in the visible region. The band at 198 nm was attributed to an aromatic ring in the molecule. Other bands of CR dye were not observed. On irradiation along with iron powder (100 mg/L) and oxidant (APS = 200 mg/L), the destruction of the chromophore (562 nm) was completed in 60 min. The intermediate peak observed at 296 nm due to the formation of substituted aromatic derivative retained its intensity up to 3 h. On continuing the irradiation up to 5 h, degradation of the dye was completed. Similar experiments were carried out using $H_2O_2$ as an oxidant where the destruction of the chromophore was completed in 90 min and complete mineralization by 6 h. The spectroscopic study of the effluents implies the efficiency of APS compared to $H_2O_2$.

## 4. Conclusions

AFP using ZVMI was applied to degrade environmentally hazardous CR dye in an aqueous medium under acidic conditions. The influence of various reaction parameters like pH of the solution, iron dosage, effect of concentration of oxidants, influence of hydroxyl radical scavenger, concentration of the dye and the effect of various inorganic anions on the decolorization rate was investigated.

APS and $H_2O_2$ showed comparable efficiencies on the degradation rate. The decrease in degradation rate at higher iron dosage is attributed to surface precipitation of the catalyst as hydroxides during the course of the reaction, which deactivates the iron surface. The decrease in the decolorization rate in the presence of hydroxyl radical scavenger confirms the role of hydroxyl radicals in the photo-Fenton degradation mechanism. The influence of various inorganic anions that are common in industrial effluents on the decolorization mechanism is also studied. All the inorganic anions in the present study showed an inhibitive effect on the degradation rate. The results imply that higher concentrations of the carbonate ion had no effect on the degradation rate for either oxidant.

The intermediates were analyzed by UV-visible and GC-MS technique. The study was extended to industrial effluents containing CR dye which required higher iron dosage for the treatment due to the presence of inorganic ions. APS acts as a better oxidant than $H_2O_2$ in treating the effluent due to the active role of sulfate-free radicals produced by the photolysis of APS and also by the reaction of APS with iron surface which mediates the degradation along with the hydroxyl radicals.

The study introduces a novel technique to degrade azo compound by using eco-friendly iron powder as the catalyst.

## Acknowledgements

Financial assistance from the UGC Major Research Project (2007-2010), Government of India, is greatly acknowledged.

## References

[1] J. Beltran, O. Rodriguez and J.R. Dominguez, Catal. Today, 101 (2005) 389–395.
[2] H.J.H. Fenton, J. Chem. Soc., 6 (1894) 899–910.
[3] M.R. Hoffmann, M. Martin, W. Choi and D. Bahnemann, Chem. Rev., 95 (1995) 69–96.
[4] E. Olilveros, O. Legrini, M. Hohl, T. Muller and A.M. Brawn, Water Sci. Tech., 35 (1997) 223–230.
[5] A.S. Amiri, J.R. Bolton and S.R. Cater, Water Res., 31 (1997) 787–798.
[6] N.H. Ince and G. Tezcanli, Water Sci. Technol., 40 (1999) 183–190.
[7] C.L. Hsueh, Y.H. Huang, C.C. Wang and C.Y. Chen, Chemosphere 58 (2005) 1409–1414.
[8] M.S. Lucas and J.A. Peres, Dyes Pigments, 71 (2006) 236–244.
[9] N. Daneshvar and A.R. Khataee, J. Environ. Sci. Health A. Environ., 41 (2006) 315–328.
[10] S. Meric, D. Kaptan and T. Olmez, Chemosphere, 54 (2004) 435–441.
[11] I. Muthuvel and M. Swaminathan, Catal. Commun., 8 (2007) 981–986.
[12] R. Matta, K. Hanna and S. Chiron, Sci. Total. Environ., 385 (2007) 242–251.
[13] F. Lucking, H. Koser, M. Jank and A. Ritter, Water Res., 32 (1998) 2607–2614.
[14] H. Kusic, N. Koprivanac, A.L. Bozic and I. Selanec. J. Haz. Mat., 136 (2006) 632–644 (and references cited therein).
[15] J.N. Fiedor, W.D. Bostick, R.J. Jarabek and J. Farrell, Environ. Sci. Technol., 32 (1998) 1466–1473.
[16] G.R. Eykholt and D.T. Davenport, Environ. Sci. Technol., 32 (1998) 1482–1487.

[17] C.P. Huang, H.W. Wang and P. Chunchiu, Water Res., 32 (1998) 2257–2264.
[18] C. Ruangchainikom, C.H. Liao, J. Anotai and M.T. Lee, Water Res., 40 (2006) 195–204.
[19] R. Venkatpathy, D.G. Bessingpas, S. Canonica and J.A. Perlinger, Appl. Catal. B: Environ., 37 (2002) 139–159.
[20] J. Lei, C. Liu, F. Li, X. Li, S. Zhou, T.X. Liu, M. Gu and Q. Wu, J. Haz. Mat., 137 (2006) 1016–1024.
[21] A. Agarwal and P.G. Tratneyk, Environ. Sci. Technol., 30 (1996) 153–160.
[22] C. Pugarin, P. Peringer, P. Albers and J. Kiwi, J. Mol. Cat. A: Chem., 95 (1999) 61–74.
[23] D.H. Bremer, A.E. Burgess, D. Houllemare and K.C. Namkung, Appl. Cata. B: Environ., 63 (2006) 15–19.
[24] U. Pagga and D. Brown, Chemosphere, 15 (1986) 479–491.
[25] D. Brown and B. Hamberger, Chemosphere, 16 (1987) 1539–1553.
[26] H. Park and W. Choi, J. Photochem. Photobiol. A: Chem., 159 (2003) 241–247.
[27] L. Gomathi Devi and G.M. Krishnaiah, J. Photochem. Photobiol. A : Chem., 121 (1999) 141–145.
[28] J. Lee and H.H. Seliger, J. Chem. Phys., 40 (1964) 519–523.
[29] P. Papapolymerou, K. Ntampegliotis, A. Riga, V. Karayannis and B. Bontozoglou, J. Haz. Mat., 136 (2006) 75–84.
[30] S.F. Kang, C.H. Liao and M.C. Chen, Chemosphere, 46 (2002) 923–928.
[31] M. Neamtu, A. Yediler, I. Siminiceanu and A. Kettrup, J. Photochem. Photobiol. A: Chem., 161 (2003) 87–93.
[32] C.F. Baes and R.E. Mesmer, The Hydrolysis of Cations, Wiley New York, 1976.
[33] K. Barbusinski and J. Majewski, Polish J. Environ. Studies, 12 (2003) 151–155.
[34] O.S.N. Sum, J. Feng, X. Hel and P.L. Yue, Topics Catalysis, 35 (2005) 233–242.
[35] P. Neta, V. Madhavan, H. Zemel and R.W. Fessemdem, J. Am. Chem. Soc., 99 (1977) 163–164.
[36] L. Gomathi Devi, S. Girish Kumar, K. Mohan Reddy and C. Munikrishnappa, J. Haz. Mat., 164 (2009) 459–467.
[37] K. Dutta, S. Mukhopadhyay, S. Bhattacharjee and B. Chaudhuri, J. Haz. Mat., 84 (2001) 57–71.
[38] M.C. Lu, J.N. Chen and C.P. Chang, Chemosphere, 35 (1997) 2285–2293.
[39] P. Papapolymerou, K. Ntampegliotis, A. Riga, V. Karayannis and K. Soutsas, Desalination, 211 (2007) 72–86.
[40] J.D. Laat, G.L. Troung and B. Legube, Water Res., 38 (2004) 2384–2394.
[41] Y. Kaqumura, P.Y. Jian, R. Nagaishi, T. Oishi and K. Ishigure, J. Phys. Chem., 95 (1991) 4435–4439.
[42] S. Martin and H.F. Fritz, Water Res., 76 (2001) 363–370.
[43] J. Bandara and J. Kiwi, New. J. Chem., 23 (1999) 717–724.
[44] N. Chahbane, D.L. Popescu, D.A. Mitchell, A. Chanda, D. Lenior, A.D. Ryabov, K.W. Schramm and T.J. Collins, Green Chem., 9 (2007) 49–57.